Towards exact free oscillation spectra through generalised normal mode coupling

Alex Myhill* **& David Al-Attar**, Bullard Laboratories, University of Cambridge

*adcm2@cam.ac.uk

1. Motivation

- Normal modes provide some of the only direct constraints on density
- There is a lack of modern computational tools for accurate low-frequency spectra
- Self-coupling codes have significant errors (Akbarashrafi et al., 2018)

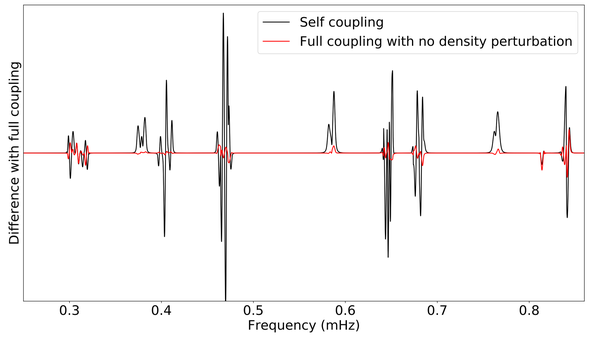

Fig. 1: Comparison of errors in self-coupling vs the size of the signal from density

- Full coupling still has approximations in both density and boundary terms (Al-Attar et al., 2018)

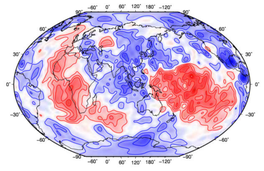

Fig. 2: Tomography model S40RTS (Ritsema et al., 2011) at the CMB

The LLSVPs are two large anomalies that consistently appear in tomography models. Their dynamic interpretation is still not fully known.
Knowledge of their density from normal mode observations is important in determining their influence.

2. Normal mode coupling

- The elastic wave equation in the frequency domain (Dahlen & Tromp, 1998)

$$\mathcal{H}\mathbf{u} + 2i\omega\boldsymbol{\Omega}\times\mathbf{u} = \omega^2\mathbf{u} \tag{1}$$

- Expanding the wavefield using the 1D normal modes as a basis yields a matrix differential equation

$$S(\omega)\mathbf{u} = -\omega^2 T\mathbf{u} + 2i\omega W\mathbf{u} + V\mathbf{u} = \mathbf{f}(\omega) \tag{2}$$

Calculating matrices

- Traditionally done uing Wigner-Eckart theorem, e.g. for kinetic energy

$$T_{k,k'} = \sum_{st}(-1)^m \left[\frac{(2l+1)(2s+1)(2l'+1)}{4\pi}\right]^{1/2} \begin{pmatrix} l & s & l' \\ -m & t & m' \end{pmatrix} \times \left\{\int_0^a \delta\tilde{\rho}_{st} T_\rho r^2 \mathrm{d}r + \sum_d d^2 \delta\tilde{d}_{st}[T_d]_-^+\right\} \tag{3}$$

- Ellipticity treated in a perturbative manner

Solving the matrix differential equation

- Non-standard eigenvalue/eigenvector problem
- Adds inaccurracy to solution for non-simple rheologies

The iterative direct solution method (IDSM) is an exact, efficient alternative suggested by Al-Attar et al. (2012), which solves for $\mathbf{u}(\omega) = S^{-1}(\omega)\mathbf{f}(\omega)$ and performs an inverse Fourier-Laplace transform

3. The referential formulation

- Mapping $\boldsymbol{\Phi}$ between geometrically spherical reference planet and physical planet

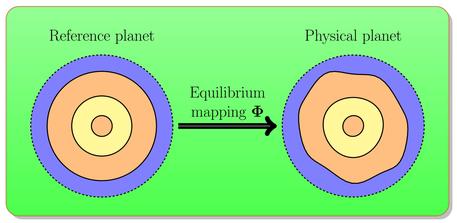

- The boundary conditions on solid-fluid boundaries are complicated

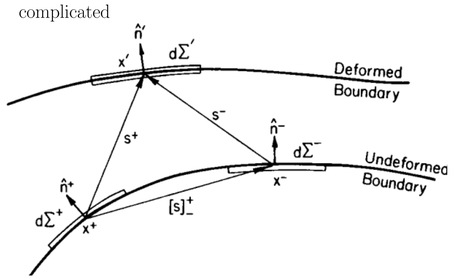

Fig. 3: Schematic of a slipping boundary from Woodhouse and Dahlen (1978)

4. Exact matrices

- Normal modes don't satisfy tangential slip condition in referential body which is

$$\left\langle (\mathrm{Def}\,\boldsymbol{\Phi})^{-1}\cdot(\mathbf{u}_2-\mathbf{u}_1), \hat{\mathbf{n}}\right\rangle = 0 \tag{4}$$

- Require the set of functions $\hat{\mathbf{u}}_n = (\mathrm{Def}\,\boldsymbol{\Phi})\cdot\mathbf{u}_n$ where $\mathbf{u}_n$ are the set of 1D normal modes
- Matrices are

$$T_{n'n} = \int_{\mathcal{M}} \rho\langle\hat{\mathbf{u}}_n, \hat{\mathbf{u}}_{n'}\rangle \mathrm{d}^3\mathbf{x} \tag{5}$$

$$W_{n'n} = \int_{\mathcal{M}} \rho\langle\boldsymbol{\Omega}\times\hat{\mathbf{u}}_n, \hat{\mathbf{u}}_{n'}\rangle \mathrm{d}^3\mathbf{x} \tag{6}$$

$$\begin{aligned} V_{n'n} = &\int_{\mathcal{M}} \{\rho\langle\boldsymbol{\Omega}\times(\boldsymbol{\Omega}\times\hat{\mathbf{u}}_n) - \boldsymbol{\gamma}_n, \hat{\mathbf{u}}_{n'}\rangle \\ &+ \langle\boldsymbol{\Lambda}\cdot\mathrm{Def}\,\hat{\mathbf{u}}_n, \mathrm{Def}\,\hat{\mathbf{u}}_{n'}\rangle\}\mathrm{d}^3\mathbf{x} \\ &+ \int_\Sigma \varpi\langle Q\cdot[\hat{\mathbf{u}}_n]_-^+, \mathrm{Def}\,\hat{\mathbf{u}}_{n'}]_-\rangle \mathrm{d}S \\ &+ \int_\Sigma \varpi\left\langle \mathrm{Def}\,\hat{\mathbf{u}}_n]_-, Q\cdot[\hat{\mathbf{u}}_{n'}]_-^+, \right\rangle \mathrm{d}S \\ &- \int_\Sigma \varpi\langle S\cdot[\hat{\mathbf{u}}_n]_-^+, [\hat{\mathbf{u}}_{n'}]_-^+\rangle \mathrm{d}S \end{aligned} \tag{7}$$

- We need to be able to solve exactly for the gravitational potential and its perturbation under motion
- The form of the matrix equations is still the exact same, ie the second part of the problem is unaffected and the IDSM can be used
- Calculation of matrix elements will be done via "spectral" method (Lognonné & Romanowicz, 1990)

5. Gravitational potential

- Weak form for the gravitational potential ζ defined on the reference body with χ as the test function is (Maitra & Al-Attar, 2019)

$$\begin{aligned} \mathcal{A}(\zeta,\chi) &= \int_{\mathcal{B}} \langle a\nabla\zeta, \nabla\overline{\chi}\rangle \mathrm{d}^3x + \sum_{lm}(l+1)b\zeta_{lm}(b)\overline{\chi_{lm}(b)} \\ &= -4\pi G\int_{\mathcal{M}} \rho\overline{\chi}\mathrm{d}^3x \end{aligned} \tag{8}$$

- $a = JF^{-1}F^{-T}$ where $F_{ij} = \partial\xi_i/\partial x_j$ and $\boldsymbol{\xi}$ maps the referential to the physical body
- Separate into a radial and a spherical harmonic basis, ie

$$\zeta(r,\theta,\varphi) = \sum_{n=1}^{N}\sum_{l=0}^{L}\sum_{m=-l}^{l} \zeta_{lmn}h_n(r)Y_{lm}(\theta,\varphi) \tag{9}$$

- Solve without deriving the matrix $A_{ij} = \mathcal{A}(\chi_i,\chi_j)$
- Uses generalised spherical harmonic (GSPH) transforms
- Motion is a perturbation to the equilibrium mapping

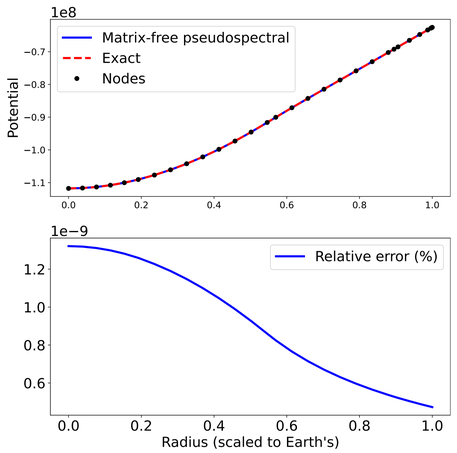

Fig. 4: Benchmark of matrix-free pseudospectral scheme against integral solution for the potential within the PREM model

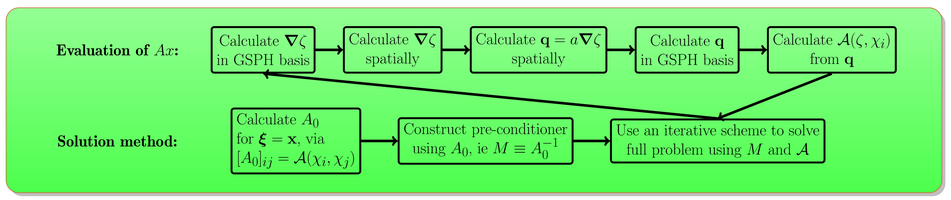

6. Improving the IDSM

- The IDSM enables rapid, accurate computation
- Decompose $S(\omega) = S_0(\omega)\tilde{S}(\omega)$ for which $S \approx S_0$ and S_0 is easily invertible
- Matrix-free iterative scheme ensures parallelisation performed with minimal memory usage increase via

$$S(\omega)\mathbf{u} = -\omega^2(T\mathbf{u}) + 2i\omega(W\mathbf{u}) + V\mathbf{u} \tag{10}$$

- BiCGSTAB and improved parallelisation result in significantly more rapid code

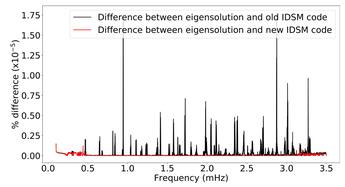

Fig. 5: Difference between IDSM and eigensolution

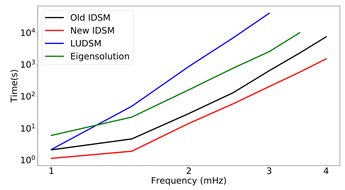

Fig. 6: Comparison of time scaling for various solvers

7. Future work

- Matrix elements for referential formulation to be calculated
- Set of basis functions cannot just be normal modes of 1D Earth
- Fully matrix-free implementation possible—efficiency and memory benefits for large coupling calculations
- Benchmarks:
  - (a) Traditional normal-mode codes with small density and topography variations
  - (b) Self-benchmarks with different $\boldsymbol{\Phi}$
- Implement adjoint calculations

Acknowledgements

- AM acknowledges the support of a NERC DTP grant and a Gates Cambridge Scholarship

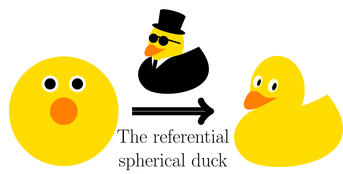

References

Akbarashrafi, F., Al-Attar, D., Deuss, A., Trampert, J., & Valentine, A. (2018). Exact free oscillation spectra, splitting functions and the resolvability of earth's density structure. *Geophysical Journal International, 213*(1), 58–76.

Al-Attar, D., Crawford, O., Valentine, A. P., & Trampert, J. (2018). Hamilton's principle and normal mode coupling in an aspherical planet with a fluid core. *Geophysical Journal International, 214*(1), 485–507.

Al-Attar, D., Woodhouse, J. H., & Deuss, A. (2012). Calculation of normal mode spectra in laterally heterogeneous earth models using an iterative direct solution method. *Geophysical Journal International, 189*(2), 1038–1046.

Dahlen, F., & Tromp, J. (1998). Theoretical global seismology. In *Theoretical global seismology*. Princeton university press.

Lognonné, P., & Romanowicz, B. (1990). Modelling of coupled normal modes of the earth: The spectral method. *Geophysical Journal International, 102*(2), 365–395.

Maitra, M., & Al-Attar, D. (2019). A non-perturbative method for gravitational potential calculations within heterogeneous and aspherical planets. *Geophysical Journal International, 219*(2), 1043–1055.

Ritsema, J., Deuss, A., Van Heijst, H., & Woodhouse, J. (2011). S40rts: A degree-40 shear-velocity model for the mantle from new rayleigh wave dispersion, teleseismic traveltime and normal-mode splitting function measurements. *Geophysical Journal International, 184*(3), 1223–1236.

Woodhouse, J. H., & Dahlen, F. A. (1978). The effect of a general aspherical perturbation on the free oscillations of the earth. *Geophysical Journal International, 53*(2), 335–354.